Available online at www.sciencedirect.com
ScienceDirect
Carbohydrate Polymers 71 (2008) 416–427
Carbohydrate Polymers
www.elsevier.com/locate/carbpol

Particulate rheology and acid-induced gelation of oxidised cellulose

Agoub A. Agoub, Edwin R. Morris *

Department of Food and Nutritional Sciences, University College Cork, Cork, Ireland

Received 15 March 2007; accepted 14 June 2007
Available online 21 June 2007

Abstract

The rheological properties of a commercial preparation of microdispersed oxidised cellulose (MDOC) from Alltracel Pharmaceuticals have been explored as background to potential applications in functional foods. In the sample studied ~85% of the particles had diameter <30 μm, with ~40% below 5 μm, ~75% of the glucose residues were converted to glucuronate, and solubility was restricted by Ca^{2+} cations present in the particles at 2:1 equivalent ratio with Na^{+}. Aqueous dispersions of MDOC were pourable, but gave gel-like mechanical spectra at concentrations far below those required for close-packing, indicating formation of a "weak gel" structure by association (adhesion) of the particles. The critical concentration (c_o) for network formation ($G' > G''$) by freshly prepared dispersions was ~4.0 wt%; at values of concentration (c) well above c_o, G' showed the c^2-dependence commonly seen for gelling biopolymers. Appreciable increases in moduli were observed on holding (15 h at 20 °C), particularly at low concentrations, consistent with progressive association. The "weak gel" networks remained intact when subjected to small stresses (<1.1 Pa at $c = 5$ wt % and <13 Pa at $c = 10$ wt%), but ruptured and flowed in response to higher stress. Breakdown of network structure occurred as a progressive process, beginning when the strain generated by applied stress exceeded a threshold value of ~50%. Dispersions prepared at concentrations below c_o had very low viscosities (e.g. ~0.01 Pa s at $c = 3$ wt%), but the effective viscosities at $c > c_o$ (attributed to re-arrangement of network structure) were massive (e.g. 10^4–10^5 Pa s at $c = 10$ wt%). A strong "true" gel structure was obtained by converting MDOC to the water-soluble sodium salt form and reducing pH with D-glucono-δ-lactone (GDL). Gel formation is attributed to suppression of electrostatic repulsion between the polymer chains by conversion of glucuronate residues to the uncharged acid form, and began as the pH dropped below ~3.3.

Keywords: Oxidised cellulose; Rheology; Gelation; Dispersions; Creep compliance

1. Introduction

Oxidised cellulose has a long history of use in wound dressing, either as a woven fabric (Johnson & Johnson Patient Care Inc., 1989) or in powder form. It is prepared by chemical conversion of C(6) hydroxymethyl (CH_2OH) groups of native cellulose to the carboxy form (COOH or COO^{-}, depending on pH). The starting material is usually cotton, and the normal reagents are oxides of nitrogen (NO_2 or N_2O_4), although other oxidising agents can be used (Kumar & Yang, 2002). Oxidised cellulose is bioabsorbable, and is one of the most biocompatible substances known. Its effectiveness in wound repair (Ashton, 1968) increases with increasing carboxyl content, and also increases with decreasing chainlength. The degree of polymerisation may, therefore, be decreased deliberately by partial hydrolysis.

Recently, oxidised cellulose has attracted attention for its potential use as a cholesterol-lowering agent in functional foods (Food Navigator, 2005). The aim of the present investigation was to explore the rheological properties of a commercial preparation of oxidised cellulose, as background to its possible use in food products. A preliminary account of some aspects of the research has been published elsewhere (Tobin, Giannouli, Agoub, & Morris, 2004).

2. Materials and methods

The material studied was kindly provided by Alltracel Pharmaceuticals PLC, Sallynoggin, Co. Dublin, Ireland. It is described as "microdispersed oxidised cellulose", and

* Corresponding author. Tel.: +353 21 4903625; fax: +353 21 4270001.
E-mail address: ed.morris@ucc.ie (E.R. Morris).

0144-8617/$ - see front matter © 2007 Published by Elsevier Ltd.
doi:10.1016/j.carbpol.2007.06.013

marketed under the proprietary name MDOC. The following technical information was supplied by Alltracel. MDOC is prepared as a mixed calcium/sodium salt, with equal molar concentrations of calcium and sodium cations (i.e. two equivalents of Ca^{2+} for each equivalent of Na^{+}), and is supplied as a finely dispersed powder. Approximately 85% of the particles have diameter below 30 μm, with ~40% below 5 μm. These particles are insoluble in dilute mineral acid, and show little solubility in water. The carboxyl content of the sample studied (expressed as COOH, on a dry-weight basis) was ~18%, which corresponds to ~75% conversion of the glucose units of cellulose to glucuronate residues. For brevity, the particulate material, as received, will be referred to as "MDOC". All samples were prepared using distilled deionised water. D-glucono-δ-lactone (GDL) was from ADM, Ringaskiddy, Co. Cork, Ireland; hydrochloric acid and sodium hydroxide were AnalaR grade from BDH.

Dispersions of MDOC in water were prepared by mechanical stirring for 20 min at ambient temperature. For studies of acid-induced gelation, solutions of oxidised cellulose in the soluble Na^{+} salt form were prepared by the following procedure. A 5.0 wt% dispersion of MDOC was mixed with an equal volume of 0.1 N HCl, stirred for 15 min at ambient temperature, and centrifuged. The compacted pellet was re-suspended in the same volume of 0.1 N HCl, and the sample was again stirred for 15 min and centrifuged. The same procedure was used to rinse the particles of oxidised cellulose in the insoluble acid form against two changes of the same volume of water. The resulting pellet was then dispersed in water, and the sample was neutralised with 0.1 N NaOH to solubilise the polymer, and adjusted to the same volume as the original dispersion, to return the concentration to 5.0 wt%. GDL was then added as solid powder, and the samples were held for 7.5 h at 20 °C. The concentration of GDL needed to give a stable value of pH 2.5 at the end of the holding period was determined by preliminary experiments. The target pH of 2.5 was selected as well below the pK_a of glucuronic acid (~pH 3.3), and the concentration of GDL required to achieve it was found to be 9.7 wt%.

All measurements were made at 20 °C. Shear-rate dependence of viscosity for MDOC dispersions prepared at concentrations of 1.0, 3.0 and 5.0 wt% was measured on a Contraves Low Shear 30 viscometer. All other rheological measurements were made using parallel plate geometry (4 cm diameter; 0.5 mm gap) on a CarriMed CSL-100 rheometer. Samples were loaded onto the rheometer at 20 °C, and coated around their periphery with light silicone oil, to minimise evaporation.

3. Results and discussion

3.1. Oscillatory rheology of MDOC dispersions

In the first series of experiments carried out in this investigation, aqueous dispersions of MDOC, chosen to give roughly equal intervals of concentration on a logarithmic scale (3.2, 4.4, 5.0, 6.3, 8.0, 10.0 and 12.0 wt%), were characterised by low-amplitude oscillatory measurements (1% strain) of storage modulus (G'), loss modulus (G'') and complex dynamic viscosity (η^*). Fig. 1 shows the values of G' (Fig. 1a) and G'' (Fig. 1b) recorded at 1 rad s^{-1} during holding for 15 h at 20 °C. For the lowest concentration studied (3.2 wt%), the values of G' increase by about an order of magnitude over the holding period, with particularly steep increase during the first 2–3 h. Increases in G' can also be seen (Fig. 1a) for all other concentrations studied, and are accompanied (Fig. 1b) by smaller increases in G''. For both moduli, the extent of increase becomes progressively smaller as concentration is raised. These

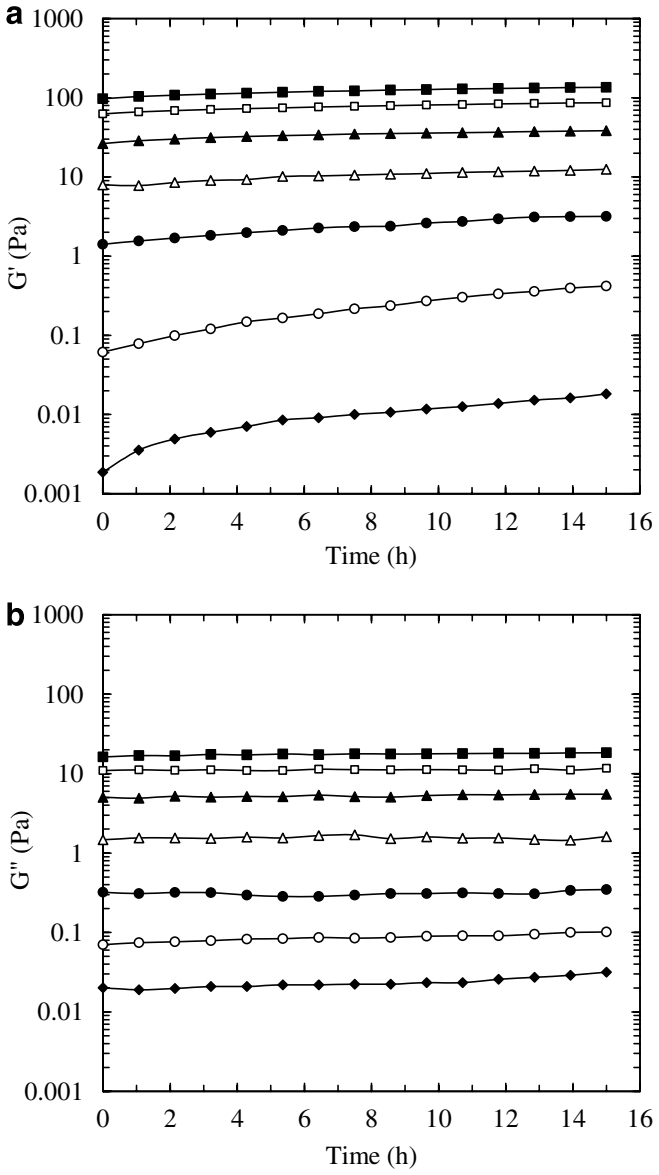

Fig. 1. Variation of (a) G' and (b) G'', measured at 1 rad s^{-1} and 1% strain, during holding at 20 °C, for MDOC dispersions at concentrations (wt%) of 3.2 (◆), 4.0 (○), 5.0 (●), 6.3 (Δ), 8.0 (▲), 10.0 (□) and 12.0 (■).

increases in moduli over time suggest development of associations between the MDOC particles.

Fig. 2 shows the values of G' and G'' at the start (Fig. 2a) and end (Fig. 2b) of the 15 h holding period (Fig. 1), plotted double-logarithmically against MDOC concentration (c). In both cases, the values of G' at concentrations above ~5 wt% are about an order of magnitude higher than the corresponding values of G'', and the slope of $\log G'$ versus $\log c$ approaches a limiting value of ~2 (c^2-dependence), behaviour typical of a crosslinked polymer network (Clark & Ross-Murphy, 1985; Ross-Murphy, 1984). For freshly prepared dispersions (i.e. measured at the start of the holding period), G' drops below G'' at ~4 wt%, indicating that this is the minimum critical concentration (c_o) at which a continuous network is formed. After 15 h at 20 °C (Fig. 2b), c_o has decreased slightly (to ~3.5 wt%), but G' at 3.2 wt% remains lower than G''.

Two concentrations of MDOC were used for investigations of network properties by creep experiments: 5 wt%, chosen as the lowest concentration at which gel-like response was observed for the freshly prepared samples in Fig. 1a, and 10 wt%, the highest concentration at which dispersions could be readily prepared using a standard laboratory stirrer. The mechanical spectra recorded for these samples, after they had been held on the rheometer for 1 h at 20 °C, are presented in Fig. 3. Both show properties characteristic (Ross-Murphy, 1984) of a continuous network ($G' > G''$; only limited variation in moduli on varying frequency). As would be expected, the moduli for the 10 wt% dispersion are consistently higher (by over an order of magnitude) than at 5 wt%. The two spectra, however, are broadly similar in form, except at high values of frequency (ω), where there is a much steeper increase in G'' at 5 wt% than at 10 wt%, indicating a higher sol-fraction of particles that are not fully connected into the network structure.

3.2. Creep-recovery studies of 10.0 wt% dispersions

In the experiments reported in this section, 10.0 wt% dispersions of MDOC (20 °C) were subjected to an applied shear stress (τ), which was held constant for a 10 min "creep period", and the resulting values of strain (γ) were measured. The stress was then removed, and measurements of strain were continued over a further 10 min "recovery period". The values of applied stress (Pa) used were 0.16,

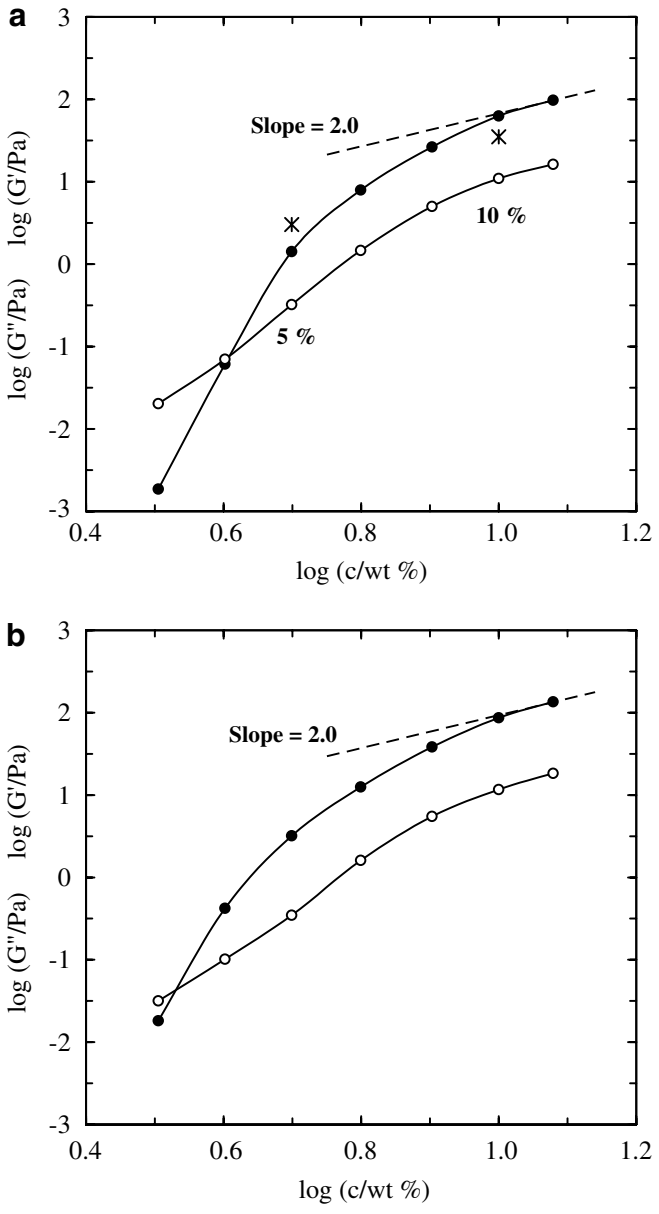

Fig. 2. Concentration-dependence of G' (●) and G'' (○) values from (a) the start and (b) the end of the 15 h holding period in Fig. 1. The asterisks at 5 and 10 wt% in (a) show the values of shear modulus (G) obtained from the strain–stress curves in Figs. 6 and 11.

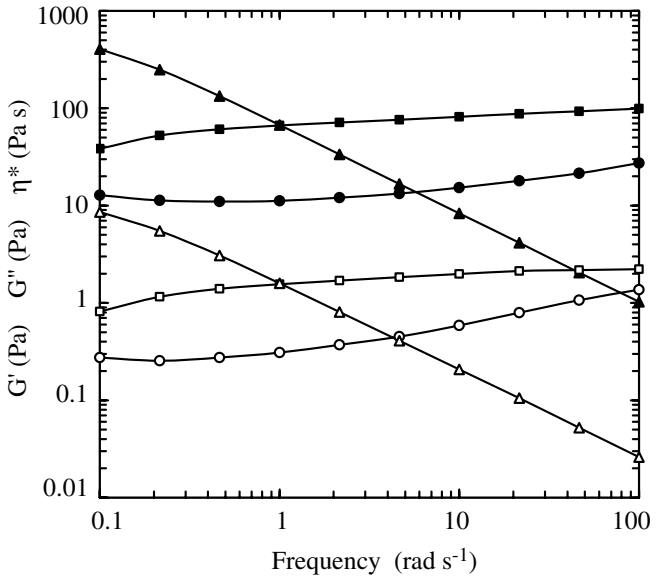

Fig. 3. Mechanical spectra (20 °C; 1% strain) showing the frequency-dependence of G' (squares), G'' (circles) and η^* (triangles) for MDOC dispersions prepared at 5.0 wt% (open symbols) and 10.0 wt% (filled symbols).

0.32, 0.64, 1.00, 1.25, 2.5, 5, 10, 11, 12, 13, 14, 15 and 17. The strains reached at the initial 10 min creep period (γ_{10}) are shown in Fig. 4, plotted double-logarithmically against applied stress. At stress values up to ~11 Pa there is a linear relationship between $\log\gamma_{10}$ and $\log\tau$, with a slope of ~1.0, which corresponds to a linear increase in γ_{10} with increasing τ ($\log\gamma_{10} = \log k + \log\tau \therefore \gamma_{10} = k\tau$). However, at higher values of applied stress, in the range 12–17 Pa, γ_{10} increases abruptly, by more than five orders of magnitude, indicating fracture of network structure.

Fig. 5 shows the creep-recovery curve recorded for an applied stress of 10 Pa, just below the range of the steep increase in γ_{10} (Fig. 4). When the stress is applied, there is a sharp initial increase in strain, as would be seen for deformation of an elastic solid. This, however, is followed by a progressive increase, with the variation of strain versus time becoming linear, as would be seen for a viscous liquid. When the stress is removed, there is a sharp reduction in strain, demonstrating survival of an elastic network with solid-like properties. At the end of the recovery period, however, there is still a large residual ("irrecoverable") strain, which can be attributed to re-arrangement of network structure during the creep period (i.e. corresponding to the progressive increase in strain in response to the applied stress). The elastic response of the network can be characterised by the "recoverable strain", determined by subtracting the residual strain at the end of the recovery period from the maximum strain reached at the end of the creep period.

As would be expected for an elastic network, there is a direct linear relationship (Fig. 6) between recoverable strain and applied stress up to the onset of fracture at ~12 Pa (Fig. 4). The reciprocal of the slope of the strain–stress curve in Fig. 6 gives the elastic (shear) modulus (G = stress/strain). As shown in Fig. 2a, the resulting value is in reasonable, although not exact, agreement with the value of G' (1 rad s^{-1}; 1% strain) for the same sample (10.0 wt% MDOC).

Fig. 7 shows the creep-recovery curves for 10.0 wt% MDOC, plotted as compliance (J = strain/stress) to facilitate comparison of response to the wide (>100-fold) range of applied stresses used (0.16–17 Pa). At the lower end of this range, from 0.16 to 5.0 Pa, there was no systematic variation in the plots of J versus time; as shown in Fig. 7a, the values of J obtained at 0.16 Pa superimpose closely on those obtained at 5 Pa, although the experimental scatter is much greater due to the much smaller strains generated. At applied stresses between 10 and 12 Pa (i.e. immediately

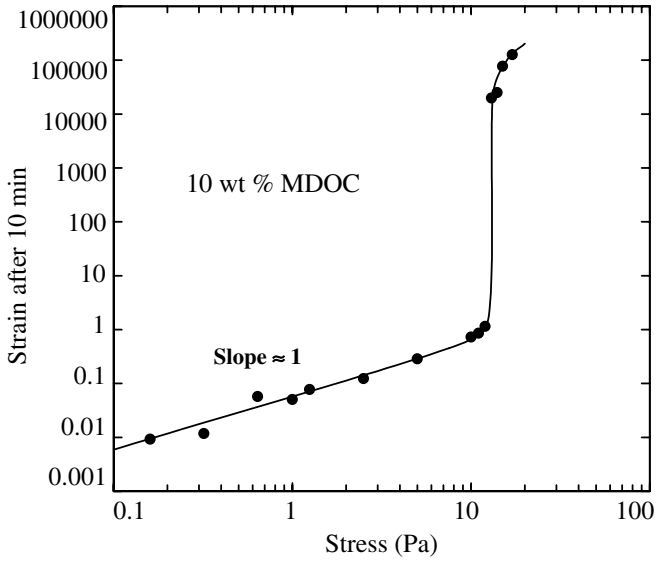

Fig. 4. Effect of applied stress on the strain reached by 10.0 wt% MDOC dispersions at the end of a 10 min creep period (at 20 °C).

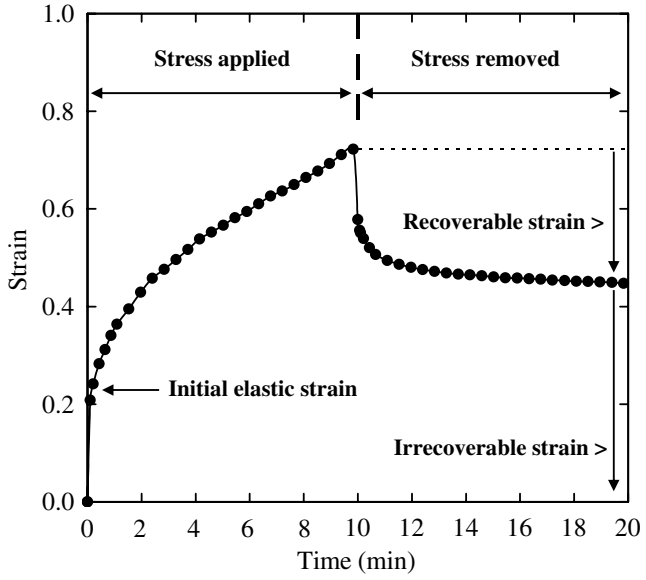

Fig. 5. Creep-recovery curve (20 °C) for 10.0 wt% MDOC at an applied stress of 10 Pa.

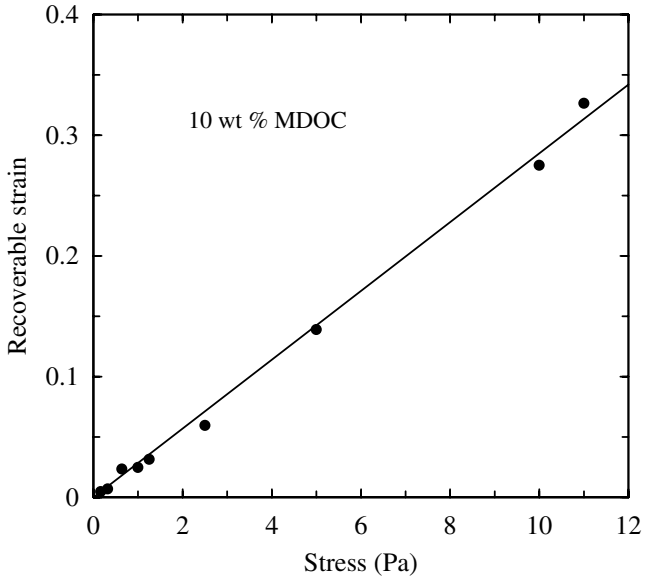

Fig. 6. Variation of recoverable strain with applied stress for 10.0 wt% MDOC at 20 °C.

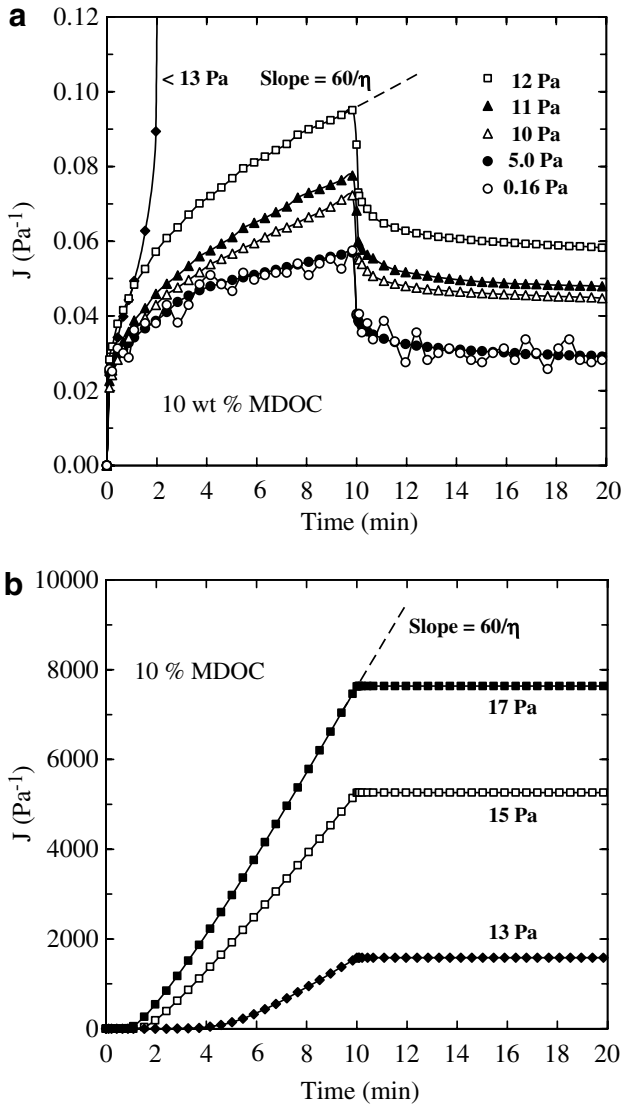

Fig. 7. Creep-recovery curves (20 °C) for 10.0 wt% MDOC at applied stress values (Pa) of 0.16 (○), 5 (●), 10 (Δ), 11 (▲), 12 (□), 13 (◆), 15 (□) and 17 (■) over (a) low and (b) high ranges of compliance (J).

before the steep increase of γ_{10} in Fig. 4) there is a progressive increase in compliance values (Fig. 7a) above those at 5 Pa, and at 13 Pa the values rise steeply above those recorded at all lower stresses. Fig. 7b shows the time-dependence of compliance at 13 Pa plotted on a greatly expanded vertical scale, along with the corresponding curves at 15 and 17 Pa. All three traces show a steep increase in compliance, which occurs at progressively shorter times as the applied stress is increased, with the curves then becoming linear, as would be observed for flow of a viscous liquid. When the stress is removed, there is no detectable decrease in strain, which is again typical of liquid-like response, and contrasts with the elastic recovery observed (Fig. 7a) at applied stresses of 12 Pa or lower. These results demonstrate that the network structure formed by 10.0 wt% dispersions of MDOC is broken down when subjected to stresses above ~12 Pa.

The early stages of breakdown are illustrated in Fig. 8, which shows the strains generated over the first 3 min of creep in response to applied stresses of 10, 12, 13, 14, 15 and 17 Pa. At 10 and 12 Pa, there is a progressive reduction in slope, towards the linear variation observed (Fig. 7a) at longer times. The curves recorded at higher values of applied stress also show an initial reduction in slope, but then pass through a point of infection, beyond which strain increases steeply. For the stresses at which this behaviour was observed (13–17 Pa), the inflection occurs at about 50% strain ($\gamma \approx 0.5$), indicating that this is the extent of deformation needed to initiate breakdown of network structure.

The effective viscosity generated by the 10.0 wt% MDOC dispersions can be determined from the slope (S) of the linear regions in the creep curves (Fig. 7): $S = \Delta J/\Delta t$; thus since $\Delta J = \Delta\gamma/\tau$, $S = (\Delta\gamma/\Delta t)/\tau$; $\Delta\gamma/\Delta t$ = shear rate ($\dot{\gamma}$); thus $S = \dot{\gamma}/\tau$, which is the reciprocal of viscosity ($\eta = \tau/\dot{\gamma}$); thus $S = 1/\eta$. For clarity of presentation, the values of time in Fig. 7 are expressed in minutes, and the above analysis would, therefore, give viscosity in units of Pa min. These can be converted to conventional units of Pa s by multiplying by 60, giving the final relationships $\eta = 60/S$; $S = 60/\eta$. The resulting values of viscosity (η/Pa s) are shown in Fig. 9. At applied stresses up to ~12 Pa where, as discussed above, flow occurs by re-arrangement of network structure, the viscosities are massive, in the range 10^4–10^5 Pa s. At higher stresses, where the network is broken and particles can move individually, the viscosities are about five orders of magnitude lower.

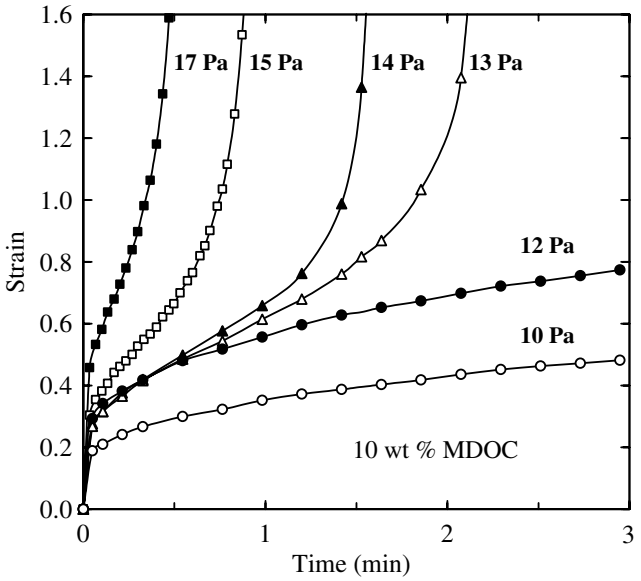

Fig. 8. Changes in strain during the first 3 min of the creep period shown in Fig. 7, for 10.0 wt% MDOC at applied stress values (Pa) of 10 (○), 12 (●), 13 (Δ), 14 (▲), 15 (□) and 17 (■).

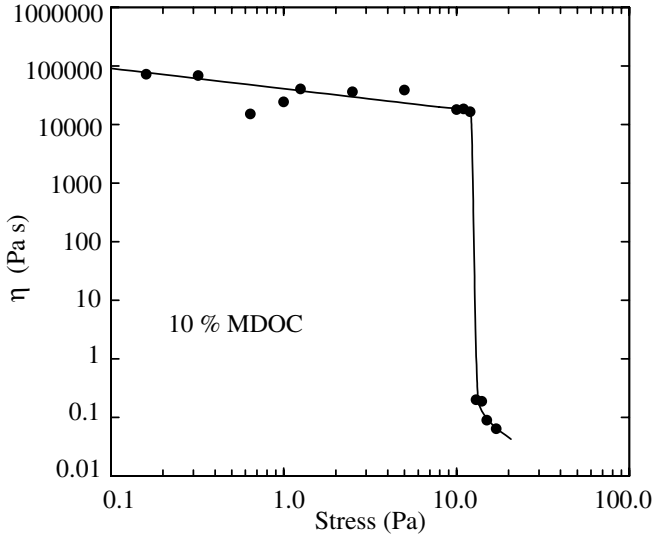

Fig. 9. Effect of stress applied to 10.0 wt% MDOC on effective viscosity (η), as determined from the slope of the linear regions in creep curves (Fig. 7).

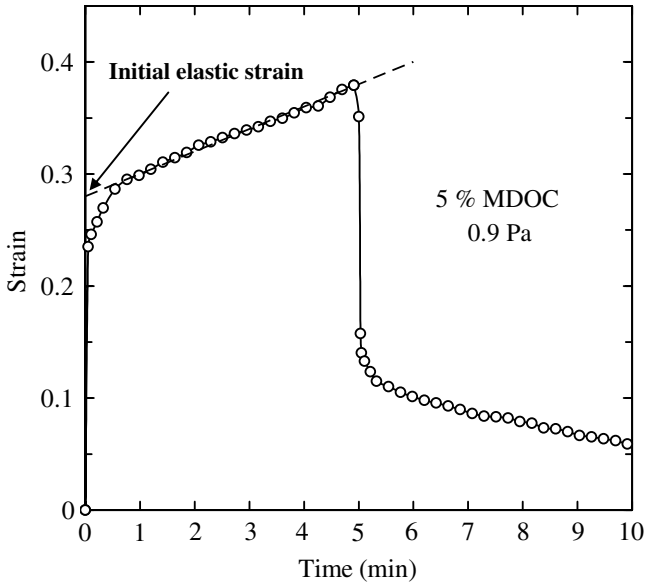

Fig. 10. Creep-recovery curve (20 °C) for 5.0 wt% MDOC at an applied stress of 0.9 Pa.

3.3. Creep response of 5.0 wt% dispersions

Dispersions of MDOC prepared at the lower concentration of 5.0 wt% also gave creep curves indicating network structure that re-arranged in response to low stresses and fractured at higher stress, but, as described below, the stress required to break the network was more than an order of magnitude lower than for the 10.0 wt% dispersions. The values of applied stress used were 0.2, 0.5, 0.9, 1.0, 1.1, 1.2, 1.3 and 1.4 Pa. Preliminary experiments showed that linear increases in strain occurred at much shorter times than at 10 wt%, and the creep and recovery periods were reduced to 5 min.

Fig. 10 shows the creep-recovery trace recorded for an applied stress of 0.9 Pa; similar curves were obtained at the two lower stresses used (0.2 and 0.5 Pa). Linear increase in strain begins well within the first minute of the creep period, and the initial elastic deformation was estimated by extrapolating the linear region to $t = 0$.

As shown in Fig. 11, the values of initial strain determined in this way for applied stresses of 0.2, 0.5 and 0.9 Pa are in good agreement with the corresponding values of recoverable strain, as would be expected for deformation of an elastic network, and both increase linearly with applied stress, which is also typical of elastic response. As found for the 10.0 wt% dispersions, the shear modulus (G) obtained from the reciprocal slope of the strain–stress curve in Fig. 11 is in reasonable, though not exact, agreement (Fig. 2a) with G' for the same sample (5.0 wt% MDOC).

Fig. 12 shows the compliance values obtained at applied stresses of 0.2, 0.5, 0.9, 1.0 and 1.1 Pa. At the first three stresses, the curves superimpose closely, as observed (Fig. 7a) for the 10.0 wt% dispersions at stresses in the range 0.16–5.0 Pa. At 1.0 Pa, however, there is a steep

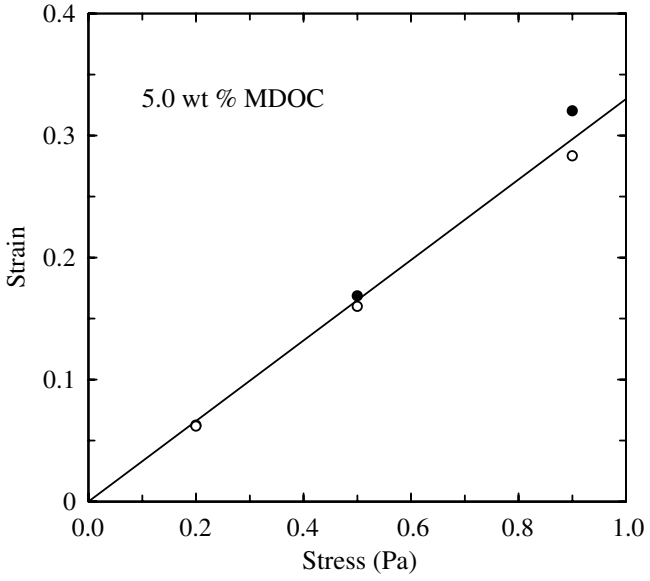

Fig. 11. Variation of initial elastic strain (○) and recoverable strain (●) with applied stress for 5.0 wt% MDOC at 20 °C.

increase in compliance over the second half of the creep period, suggesting the onset of network breakdown, and at 1.1 Pa the values rise sharply above those recorded at lower stress. As illustrated in Fig. 13, the accelerating increase in rate of deformation (flow) seems to begin when the strain reaches a value of ~0.5, as was also observed (Fig. 8) for the 10.0 wt% dispersions.

Fig. 14 shows the strains generated over the first 60 s of the creep period in response to applied stresses of 1.1 Pa (Fig. 14a), the first value at which a massive increase in compliance was observed (Fig. 12), and 1.4 Pa (Fig. 14b), the maximum stress used. In both cases, the linear increase in strain over time, characteristic of viscous flow, occurs

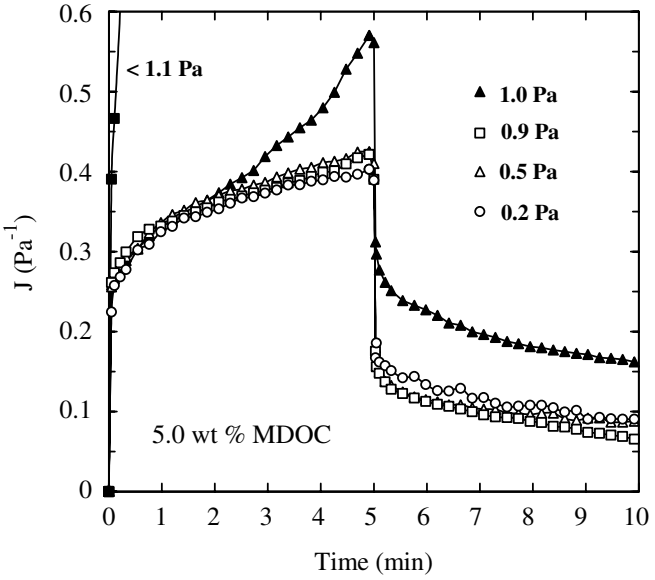

Fig. 12. Creep-recovery curves (20 °C) for 5.0 wt% MDOC at applied stress values (Pa) of 0.2 (○), 0.5 (Δ), 0.9 (□), 1.0 (▲) and 1.1 (■).

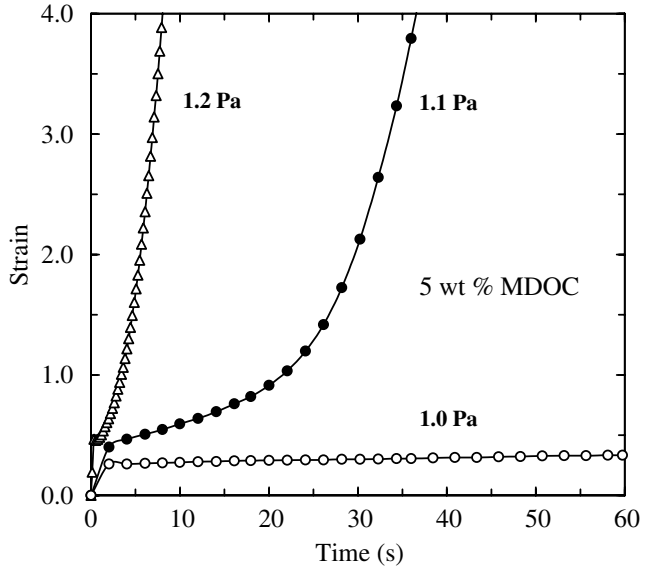

Fig. 13. Changes in strain during the first 60 s of the creep period shown in Fig. 12, for 5.0 wt% MDOC (20 °C) at applied stress values (Pa) of 1.0 (○), 1.1 (●) and 1.2 (Δ).

within this brief period of applied stress. Similar curves were obtained at intermediate stresses (1.2 and 1.3 Pa).

3.4. Rheological comparisons

The results from the creep experiments demonstrate breakdown of network structure when stress exceeds a threshold value, which for the 5.0 wt% dispersions appears to occur (Fig. 12) at ~1.1 Pa. An alternative, and potentially simpler, way of determining the stress required to fracture a weak, continuous network, however, is to apply a programmed increase in stress and observe the value at

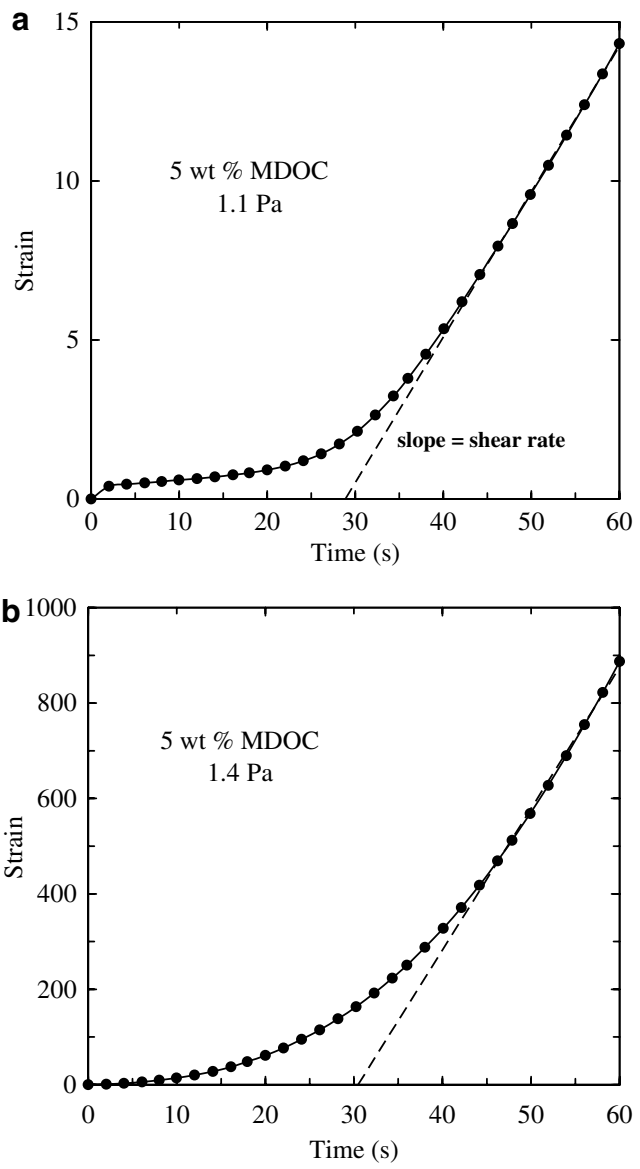

Fig. 14. Changes in strain during the first 60 s of the creep period shown in Fig. 12, for 5.0 wt% MDOC (20 °C) at applied stress values of (a) 1.1 Pa and (b) 1.4 Pa.

which flow begins. Fig. 15 shows the shear rates generated in a 5.0 wt% MDOC dispersion as stress was increased linearly from 0 to 2 Pa over a period of 2 min. Up to ~1 min the shear rates remain extremely low, indicating that they arise from re-arrangement of network structure, but there is then a fairly sharp transition to a linear increase in shear rate ($\dot{\gamma}$) with increasing stress, as would be expected from fracture of the network and subsequent flow of the constituent particles. The stress at the point of fracture (“break stress”) can be estimated by extrapolation of the linear region to $\dot{\gamma} = 0$.

Similar curves were obtained (Fig. 16a) when stress was increased from 0 to 2 Pa over progressively longer periods of time (5, 10 and 15 min), but with a systematic increase in the extrapolated values of break stress. A likely explanation is that the more slowly stress is increased, the more

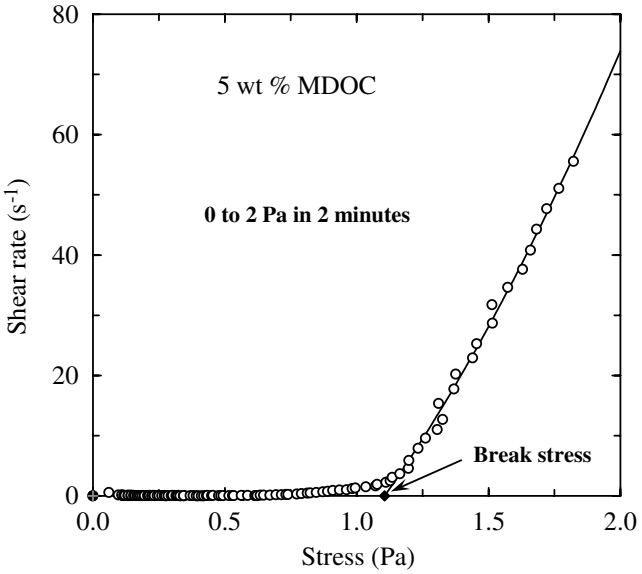

Fig. 15. Determination of break stress from the shear rates generated in 5.0 wt% MDOC (20 °C) on increasing stress from 0 to 2 Pa over a period of 2 min.

time there is for the network to respond by re-arranging rather than breaking. Fig. 16b shows the break stress values from Fig. 16a plotted against $\Delta t/\Delta\tau$ (i.e. as the reciprocal of the rate of increase in stress). The plot is reasonably linear, and extrapolates to a break stress of ~1.1 Pa at $\Delta t/\Delta\tau = 0$ (which corresponds to instantaneous application of stress). This is in excellent agreement with the creep experiments, where stress is applied almost instantaneously, which also showed network fracture at ~1.1 Pa (Figs. 12 and 13) for the same sample.

Fig. 17 shows the shear-rate dependence of viscosity (from rotational measurements) for MDOC dispersions prepared at concentrations of 1.0, 3.0 and 5.0 wt%. At 1.0 wt%, the flow curve is horizontal (i.e. Newtonian), and the viscosity is less than twice that of water. At 3.0 wt%, there is a significant reduction in viscosity with increasing shear rate (''shear thinning''), and the viscosity values are about an order of magnitude higher than at 1.0 wt%. On further increase in concentration to 5.0 wt%, the viscosity values again increase by about an order of magnitude, with an accompanying increase in extent of shear thinning.

As reported in Section 3.3, the creep curves of strain (γ) versus time (t) for 5.0 wt% MDOC dispersions at applied stresses of 1.1 Pa and above (1.2, 1.3 and 1.4 Pa) became linear (Fig. 14) within the first 60 s of the creep period. The slope of this linear region gives the shear rate ($\dot{\gamma} = \Delta\gamma/\Delta t$) generated in response to the applied stress (τ), and hence the viscosity ($\eta = \tau/\dot{\gamma}$). The values of shear rate and viscosity obtained in this way are shown in Fig. 18, in comparison with the shear-rate dependence of viscosity from rotational measurements (Fig. 17) and frequency-dependence of complex dynamic viscosity (η^*; Fig. 3) for the same sample (5.0 wt% MDOC).

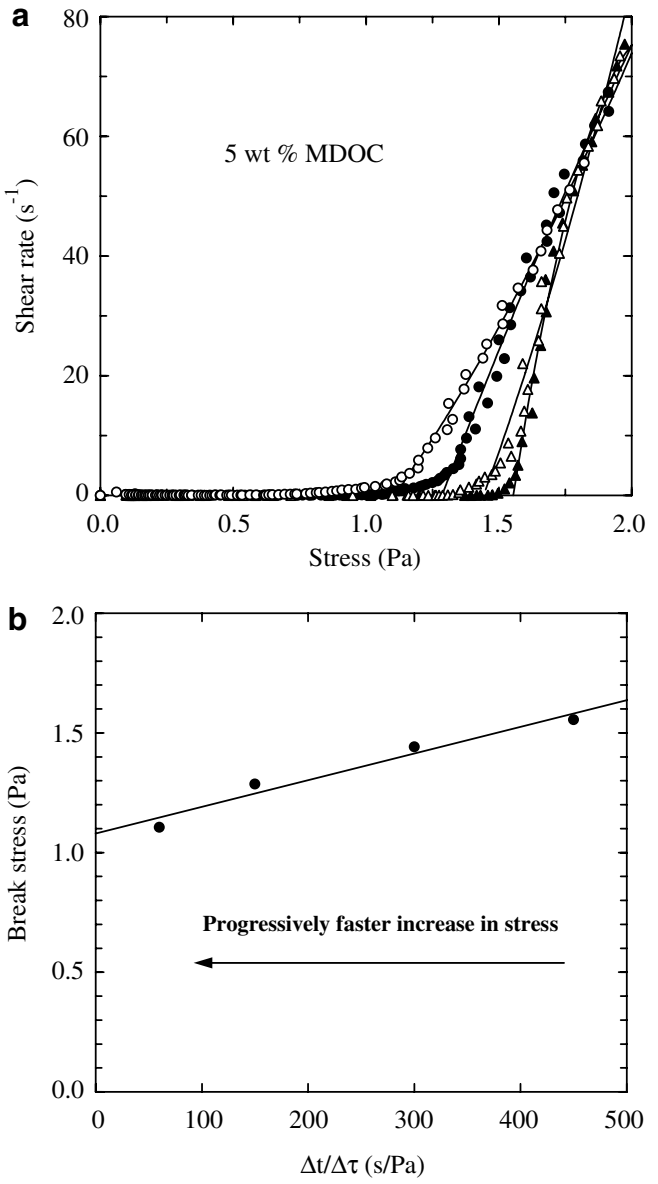

Fig. 16. (a) Shear rates generated in 5.0 wt% MDOC (20 °C) on increasing stress (τ) from 0 to 2 Pa over periods of 2 (○), 5 (●), 10 (Δ) and 15 (▲) min. (b) Variation of break stress values estimated (Fig. 15) from the curves in (a), with the reciprocal of the rate of increase in stress ($\Delta t/\Delta\tau$).

For simple liquids and solutions of disordered polymers, the variation of η^* with frequency (ω/rad s^{-1}) superimposes closely on the variation of rotational viscosity (η) with shear rate ($\dot{\gamma}$/s^{-1}). This generality is known as the ''Cox-Merz'' rule (Cox & Merz, 1958). However, the 5.0 wt% MDOC dispersions violate the Cox-Merz rule: η^* from low-amplitude oscillatory measurements is consistently higher (Fig. 18) than η from rotational measurements at equivalent values of frequency and shear rate. Similar behaviour is observed for other materials which, like the MDOC dispersions, show gel-like response to small-deformations but flow in response to higher stresses. Materials of this type are known as ''weak gels'' (Ross-Murphy, 1984), and their departure from Cox-Merz superposition

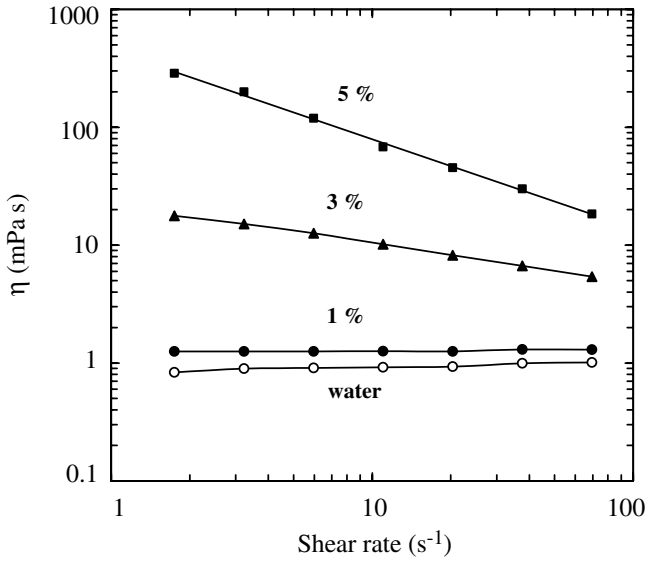

Fig. 17. Shear-rate dependence of viscosity (20 °C) for water (○) and for MDOC dispersions prepared at concentrations (wt%) of 1.0 (●), 3.0 (▲) and 5.0 (■).

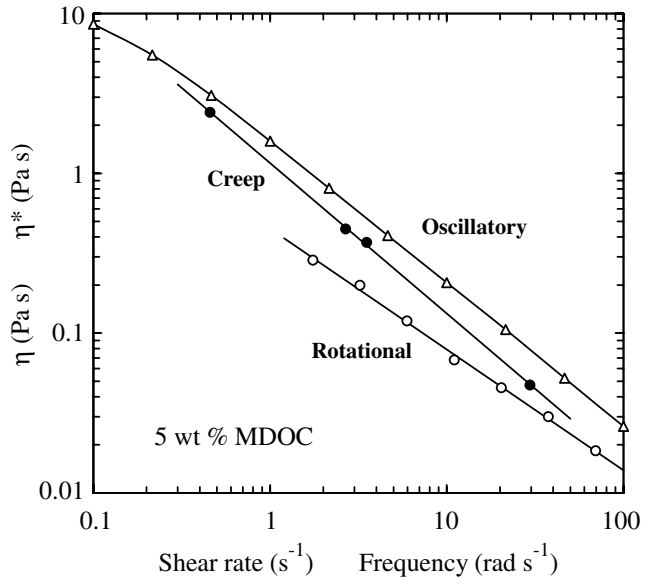

Fig. 18. Comparison of values of apparent viscosity (●) calculated from the slope of strain–time curves (Fig. 14) from creep experiments with the frequency-dependence of η^* (Δ) from small-deformation oscillatory measurements and shear-rate dependence of η (○) from rotational measurements (Fig. 17) for 5.0 wt% MDOC (20 °C).

of η and η^* can be readily explained. The values of η^* from small-deformation measurements characterise the response of the intact "weak gel" network; rotational measurements, by their nature, cause breakdown of network structure, and the lower values of η characterise flow of the resulting fragments.

As shown in Fig. 18, the values of apparent viscosity derived from the creep experiments (Fig. 14) lie between the curves obtained from oscillatory and rotational measurements. At low shear rate, they are close to the corresponding values of η^*, but then drop towards the rotational values of η as shear rate increases in response to increase in applied stress (1.1–1.4 Pa), indicating progressive breakdown of network fragments.

3.5. Acid-induced gelation

The investigation reported in this section was confined to a single concentration (5.0 wt%) of oxidised cellulose, after conversion to the soluble sodium salt form. As described in Section 2, acidification to a pH of 2.5 was induced by incorporation of 9.7 wt% GDL and holding for 7.5 h at 20 °C. The progressive reduction in pH to the final stable value of 2.5 is shown in Fig. 19.

Fig. 20 shows the accompanying changes in G' and G'', plotted against holding time expressed linearly (Fig. 20a) and logarithmically (Fig. 20b). Over about the first half-hour of the holding period there is little detectable change in G'', and G' is too low to be measured (<0.01 Pa). There is then, however, a steep increase in both moduli, with G' rising above G''. The curves cross at a holding time of ~45 min, which can therefore be regarded as the point at which the initial solution forms a continuous network (i.e. the critical gel point). At longer times, the moduli continue to rise, but then level out to constant values after ~4 h of holding at 20 °C, which corresponds to the time at which reduction in pH (Fig. 19) is essentially complete. The variation of G' and G'' (Fig. 20) with pH (Fig. 19) is shown directly in Fig. 21. Gelation ($G' > G''$) occurs at ~pH 3.3, the pK_a of glucuronic acid (Morris, Rees, Sanderson, & Thom, 1975), with progressive increase in moduli on further decrease in pH.

The mechanical spectrum of the gel network at the end of the holding period, when pH had reached the final stable

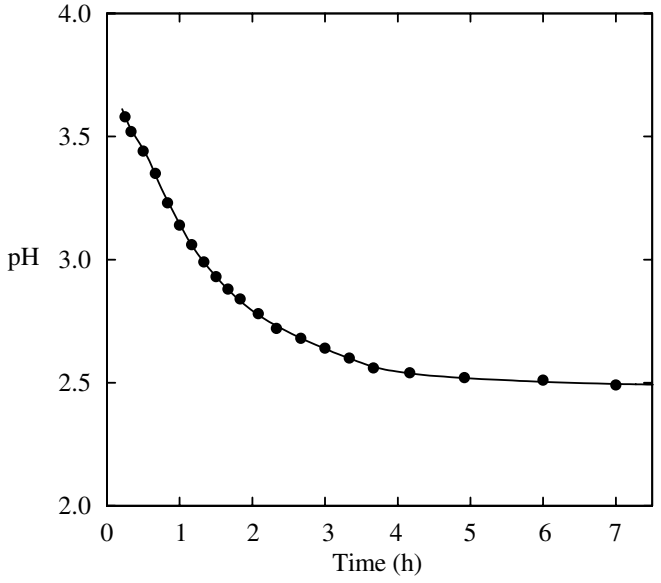

Fig. 19. Reduction in pH over time for 5.0 wt% oxidised cellulose (Na^+ salt form) in the presence of 9.7 wt% GDL at 20 °C.

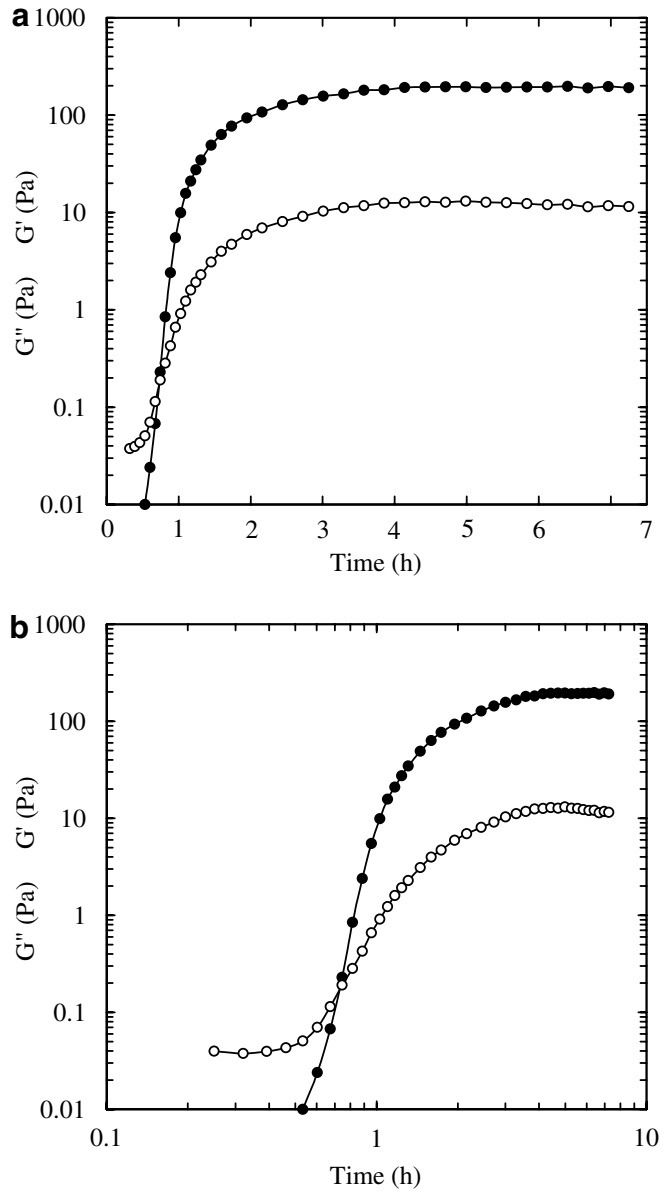

Fig. 20. Changes in G' (●) and G'' (○), measured at 1 rad s^{-1} and 1% strain, for 5.0 wt% oxidised cellulose (Na^+ salt form) during progressive acidification (Fig. 19) with GDL (9.7 wt%; 20 °C), plotted against time expressed (a) linearly and (b) logarithmically.

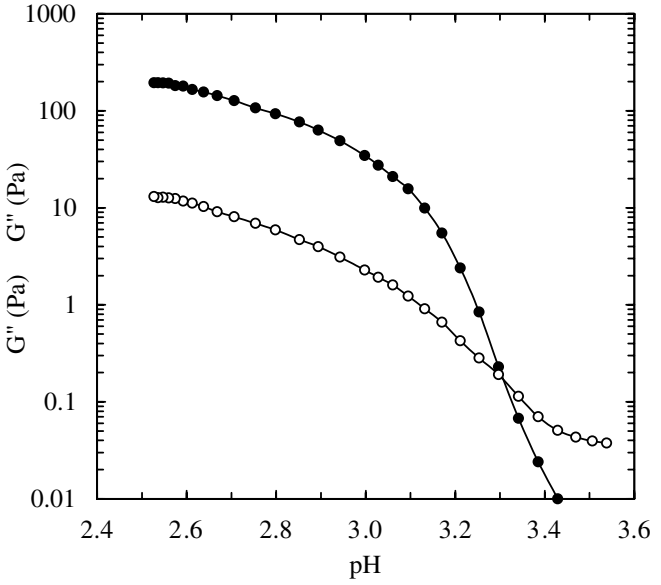

Fig. 21. Variation of G' (●) and G'' (○) with pH for 5.0 wt% oxidised cellulose (Na^+ salt form) during progressive acidification with GDL (9.7 wt%) at 20 °C.

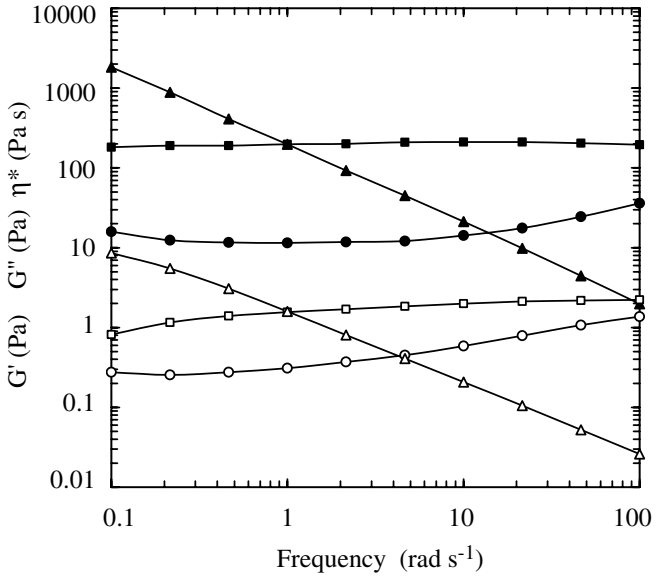

Fig. 22. Mechanical spectra (20 °C; 1% strain) showing the frequency-dependence of G' (squares), G'' (circles) and η^* (triangles) for 5.0 wt% oxidised cellulose, as a particulate MDOC dispersion (open symbols) and an acid-induced gel at pH 2.5 (filled symbols).

value of 2.5, is shown in Fig. 22, in comparison with the spectrum obtained (Fig. 3) for the same concentration (5.0 wt%) of oxidised cellulose as a particulate (MDOC) dispersion. The spectrum recorded for the dispersion is similar to those observed for "weak gels", such as the pourable networks formed by ordered xanthan (Ross-Murphy, Morris, & Morris, 1983): comparatively small separation between G' and G'', and an appreciable increase in G' with increasing frequency. The spectrum of the acidified sample, by contrast, is typical (Ross-Murphy, 1984) of a strong gel: G' is about a decade higher than G'', and virtually independent of frequency. The absolute values of both moduli for the acidified sample are around two orders of magnitude higher than those of the particulate dispersion, again demonstrating a much stronger network.

4. Conclusions

Acid-induced gelation of oxidised cellulose can be explained as follows. In native cellulose, the (1 → 4)-linked β-D-glucan chains have an extended, 2-fold conformation and are packed together in an insoluble fibrillar structure stabilised by extensive hydrogen-bonding within and

between the constituent chains (Millane, 1992). Introduction of charged groups by conversion of glucose residues to glucuronate promotes dissociation of the polymer chains by electrostatic repulsion, and can yield a soluble product. Solubility of MDOC is restricted by the presence of divalent cations (Ca^{2+}). Monovalent (Na^{+}) cations, having lower charge, are less effective in offsetting electrostatic repulsion, and allow the polyanionic chains to dissociate into the solution state. Progressive reduction in pH promotes re-association into intermolecular junctions of a gel network by converting the carboxy groups of glucuronate from the charged (COO^{-}) form to the uncharged (COOH) form, thus reducing, and, at sufficiently low pH, virtually eliminating, electrostatic repulsion.

At all concentrations studied (1–12 wt%), aqueous dispersions of MDOC remained pourable. However, as described in Sections 3.2 and 3.3, the two preparations characterised in detail (5.0 and 10.0 wt%) showed clear evidence of network structure, and can therefore be classified as "weak gels".

All particulate dispersions would be expected to develop solid-like properties at concentrations high enough for the individual particles to come into contact with one another. The results of this investigation, however, strongly indicate that the "weak gel" properties of MDOC dispersions arise from association (adhesion) of particles, rather than from simple physical contacts. The evidence pointing to this conclusion can be summarised as follows.

1. The onset of close-packing of monodisperse spherical particles occurs when the particles occupy ~65% of the total volume, and moves to progressively higher concentration (volume fraction) with increasing polydispersity. MDOC dispersions, however, gave gel-like mechanical spectra (Fig. 3) and showed elastic recovery in creep experiments (Figs. 7a, 10 and 12) at much lower concentrations (5 and 10 wt%). Even allowing for some swelling of the particles in water, the gross disparity between these concentrations and the value of ~65% required for close-packing argues against development of network structure by particles being forced into contact with one another.
2. The observed increases in moduli over time (Fig. 1) are consistent with progressive adhesion between particles, but cannot be explained by physical contacts.
3. The concentration-dependence of G' (Fig. 2) shows no evidence of the sharp increase that would be expected as particles approach close-packing, but has the form typical (Clark & Ross-Murphy, 1985) of a gelling biopolymer, with a progressive reduction in the slope of $\log G'$ versus $\log c$ towards a c^2-dependence of modulus.

The MDOC "weak gel" networks remain intact when subjected to small stresses, but break down at higher stress, and then flow like liquids. The stress required to break the network increases with increasing concentration of MDOC, from ~1.1 Pa (Figs. 12, 13, 14a and 16b) at 5.0 wt% to ~13 Pa (Figs. 4, 7 and 9) at 1.0 wt%. Breakdown of "weak gel" structure appears to occur progressively, rather than by sharp fracture of the network. At low values of applied stress, creep curves of compliance versus time superimpose closely (Figs. 7a and 12), and the progressive increase in compliance after the initial elastic deformation can be attributed to network re-arrangement by existing associations between particles coming apart and being replaced by new associations, but with no overall change in network connectivity. The first indication of reduction in association during the creep period is that the compliance curves rise above those recorded at lower stresses, but elastic recovery when the stress is removed shows survival of network structure.

On further increase in stress, there is a massive increase in the extent of deformation (Figs. 4, 7, 12 and 13), curves of stress (and hence compliance) against time become linear (i.e. characteristic of liquid flow), and there is no recovery when stress is removed (Fig. 7b), demonstrating that the continuous "weak gel" network has been destroyed. Before the linear region (Figs. 7b and 14) is reached, there is a progressive, accelerating increase in deformation over time, indicating progressive breakdown of network structure. The onset of this accelerating increase appears to occur (Figs. 8 and 13) at about 50% strain ($\gamma \approx 0.5$), suggesting that this is the maximum deformation that the "weak gel" networks can accommodate by re-arranging rather than breaking.

Progressive loss of network structure is also indicated by the curves of shear rate generated in response to a progressive increase in stress (Fig. 16a), which show a region of upward curvature before becoming linear, and by the progressive decrease (Fig. 18) of apparent viscosity derived by creep experiments at increasing stress, from values close to those of η^* (characterising the unbroken network) towards the lower values obtained by rotational measurements (which would be expected to cause extensive loss of association between particles).

As shown in Fig. 2a, the minimum concentration (c_o) required to give "weak gel" structure in freshly prepared dispersions of MDOC is ~4 wt%, decreasing to ~3.5 wt% (Fig. 2b) in samples held for 15 h at 20 °C. At lower concentrations (Fig. 17) the dispersions have very low viscosity (e.g. ~10 mPa s at 3.0 wt%), suggesting that MDOC could be incorporated in food products at concentrations in this range without causing any appreciable change in texture, which could be of advantage in applications focussed on its physiological effects. However, the "weak gel" networks formed at higher concentrations (~5 wt% and above) might, like those of xanthan (Morris, 1991), be effective in stabilising emulsions by physical trapping of oil droplets, and in preventing sedimentation of solids (pieces of fruit, vegetables, herbs, etc.) in fluid products.

Acknowledgements

We thank Dr. Brona O'Neill of Alltracel for drawing our attention to oxidised cellulose, and for arranging

supply of the sample studied. We also thank Dr. Ivan Santar, Tisnov, Czech Republic, and Dr. Robert K. Richardson, Clophill, Bedford, UK, for helpful discussions.

References

Ashton, W. H. (1968). Oxidised cellulose product and method for preparing the same. United States Patent 3, 364, 200.

Clark, A. H., & Ross-Murphy, S. B. (1985). The concentration dependence of biopolymer gel modulus. *British Polymer Journal, 17*, 164–168.

Cox, W. P., & Merz, E. H. (1958). Correlation of dynamic and steady-flow viscosities. *Journal of Polymer Science, 28*, 619–622.

Food Navigator (2005). New results back Alltracel's cholesterol-lowering compound http://www.foodnavigator.com/news/printNewsBis.asp?id=63034.

Johnson & Johnson Patient Care Inc. (1989). Surgical absorbable hemostate, PC-0506, 08901-2023, New Brunswick: NJ.

Kumar, V., & Yang, T. (2002). HNO_3/H_3PO_4–$NaNO_2$ mediated oxidation of cellulose – preparation and characterization of bioabsorbable oxidised celluloses in high yields and with different levels of oxidation. *Carbohydrate Polymers, 48*, 403–412.

Millane, R. P. (1992). Molecular and crystal structures of polysaccharides with cellulosic backbones. In R. Chandrasekaran (Ed.), *Frontiers in Carbohydrate Research 2* (pp. 168–190). New York: Elsevier.

Morris, E. R. (1991). Pourable gels: Polysaccharides that stabilise emulsions and dispersions by physical trapping. *International Food Ingredients, 1*, 32–37.

Morris, E. R., Rees, D. A., Sanderson, G. R., & Thom, D. (1975). Conformation and circular dichroism of uronic acid residues in glycosides and polysaccharides. *Journal of the Chemical Society, Perkin Transactions, 2*, 1418–1425.

Ross-Murphy, S. B. (1984). Rheological methods. In H. W.-S. Chan (Ed.), *Biophysical Methods in Food Research. Critical Reports on Applied Chemistry* (pp. 195–290). London, UK: SCI.

Ross-Murphy, S. B., Morris, V. J., & Morris, E. R. (1983). Molecular viscoelasticity of xanthan polysaccharide. *Faraday Symposia of the Chemical Society, 18*, 115–129.

Tobin, A., Giannouli, P., Agoub, A., & Morris, E. R. (2004). Creep compliance of pourable gels – new applications of an old technique. In P. A. Williams & G. O. Phillips (Eds.), *Gums and Stabilisers for the Food Industry 12* (pp. 145–152). Cambridge, UK: Royal Society of Chemistry.